Tuberculosis 119 (2019) 101880

Contents lists available at ScienceDirect

Tuberculosis

journal homepage: http://www.elsevier.com/locate/tube

Mechanisms of Pathogenesis

Characterization of a novel *Mycobacterium tuberculosis* serine protease (Rv3194c) activity and pathogenicity

He Li [a,1], Guanghui Dang [a,1], Hongxiu Liu [a], Zhongxing Wang [b], Ziyin Cui [a], Ningning Song [a], Liping Chen [a], Siguo Liu [a,*]

[a] *Division of Bacterial Diseases, State Key Laboratory of Veterinary Biotechnology, Harbin Veterinary Research Institute, Chinese Academy of Agricultural Sciences, Harbin, 150001, PR China*

[b] *College of Animal Science and Technology, Jilin Agricultural University, Changchun, PR China*

ARTICLE INFO

Keywords:
Mycobacterium tuberculosis
Serine protease
Rv3194c
Activity and pathogenicity
Mycobacterium smegmatis

ABSTRACT

Mycobacterium tuberculosis (MTB) serine proteases are important pathogen-associated virulence factors that are involved in the invasion, bacterial persistence, and degradation of host defense factors. The current study identified and characterized a novel serine protease, Rv3194c, of MTB. A heterologous Rv3194c protein, purified from *Escherichia coli*, possessed proteolytic activity that could hydrolyze bovine serum albumin (BSA), milk, casein, and gelatin at an optimal temperature of 40 °C and a pH of 8.0. Furthermore, the divalent metal ions Ca^{2+} and Mn^{2+} increased the activity of Rv3194c. Betulinic acid, a Traditional Chinese Medicine (TCM) monomer; PMSF, a chemical inhibitor; and the Roche inhibitor cocktail inhibited proteolytic activity. Site-directed mutagenesis demonstrated that D308 and particularly S309 play a crucial role in the catalytic activity of Rv3194c protease. The cellular assays revealed that Rv3194c inhibits THP1-derived macrophage migration. Moreover, Rv3194c degraded the complement components, C3b and C5a, causing inhibition of phagocytosis and chemotaxis. In mice, Rv3194c enhanced the persistence of *Mycobacterium smegmatis* (Ms) in the lung, induced lung lesions, and promoted the release of inflammatory cytokines. The results of this study indicate that Rv3194c may play an important role in the pathogenicity of mycobacteria.

1. Introduction

Mycobacterium tuberculosis (MTB), the pathogenic agent of tuberculosis (TB), is a life-threatening infectious disease. Globally, TB remains one of the top 10 causes of death and affects millions of people each year. In 2017, nearly 10 million people were estimated to have been infected with TB, and 300,000 TB-related deaths occurred in human immunodeficiency virus (HIV)-positive patients [1]. Meanwhile, the emergence of multidrug-resistance (MDR) strains in infection alone or co-infection with HIV complicates TB treatment and prevention [2]. Thus, it is vital to explore the pathogenic mechanisms of TB and identify new pathogenic factors to design novel drugs to fight TB and reduce its threat to public health.

Bacterial serine proteases are important factors involved in the invasion of mammalian cells, especially macrophages [3,4], and they can contribute to MTB virulence infection and proliferation. Many MTB serine proteases, such as Rv2869c, Rv0125c (pepA), and Rv0983c, have been identified and characterized. These serine proteases regulate mononuclear cell proliferation and inflammatory cytokine secretion and increase the virulence and persistence of MTB [5,6]. In host-pathogen interactions, serine proteases counteract the host immune responses through the cleavage of immunoglobulins and complement to escape from host immune surveillance and the manipulation of the immune cell signals to increase the proliferation of pathogens [7–9]. Rv3194c belongs to the S16 serine protease family. Bioinformatic analysis (SignalP 4.1 Server and TMHMM Server v. 2.0) has shown that 1–23 amino acids are a potential signal peptide and 1–27 amino acids are a transmembrane helix. In addition, a recent study demonstrated that Rv3194c might possess adhesion characteristics [10]. In this study, we show that Rv3194c could hydrolyze BSA, casein, gelatin, and milk *in vitro,* and inhibit THP1-derived macrophage migration and phagocytosis. In addition, Rv3194c serine protease promoted the persistence of

* Corresponding author. State Key Laboratory of Veterinary Biotechnology, Harbin Veterinary Research Institute, the Chinese Academy of Agricultural Sciences, 678 Harping Street, Harbin, 150001, Heilongjiang, PR China.
E-mail address: liusiguo@caas.cn (S. Liu).

[1] Both authors contributed equally to this work.

https://doi.org/10.1016/j.tube.2019.101880
Received 16 April 2019; Received in revised form 1 November 2019; Accepted 1 November 2019
Available online 4 November 2019

Mycobacterium smegmatis in mice and induced pathological lung injury and the release of inflammatory cytokines.

2. Materials and methods

2.1. Animals, bacterial strains, plasmids, and antibodies

Mice (5-week-old female C57BL/6 and BALB/c) and New Zealand white rabbits were purchased from Vital River (Beijing, China). Experiments involving mice were performed according to the recommendations of the Heilongjiang Animal Ethics Committee (Harbin, Heilongjiang, China). The Animal Welfare Commissioner approved the ethical guidelines. Distress was minimized in all of the experimental animals. *Mycobacterium smegmatis* (Ms) mc^2155 and bacillus Calmette-Guérin (BCG *bovis* Tokyo 172) strains were cultivated in 7H9 and 7H10 medium (BD Biosciences, San Jose, CA, USA) with 0.2% glycerol, 0.05% Tween 80 (Sigma-Aldrich, St. Louis, MO, USA), and 10% oleic acid/albumin/catalase (OADC) (BD Biosciences). The MTB (H37Rv) genome was used to amplify the *rv3194c* and *rv0983c* genes. The pMV261-AI-N vector (Supplementary data), based on the pMV261 vector backbone, was modified and used to construct recombinant plasmids. The polyclonal antibodies anti-Rv3194c and anti-KatG were prepared from BALB/c mice and rabbits, respectively. Anti-6 × His monoclonal antibody (1:5,000) from mouse (Sigma-Aldrich), goat anti-rabbit IgG Dylight 800-labeled antibody, and goat anti-mouse IgG Dylight 800-labeled antibody (1:10,000) (KPL, USA) were used for Western blotting.

2.2. Expression, purification, and identification of Rv3194c

The *rv3194c* gene from the genomic DNA of MTB H37Rv was amplified by PCR using specific primers (Supplementary Table S1). The products were digested and ligated into the pET22b vector (Novagen, Darmstadt, Germany) with a sequence encoding a 6 × His-tag on the C-terminus. The Rv3194c protein was expressed in *E. coli* BL21 and purified by affinity chromatography, gel filtration chromatography, and ion-exchange chromatography. The purified protein was analyzed by SDS-PAGE. Western blotting was also conducted to analyze Rv3194c expression with anti-6 × His and anti-Rv3194c antibodies. Finally, Rv3194c identification was completed by mass spectrometry.

2.3. Substrates for Rv3194c serine protease

Preliminary determination of the Rv3194c serine protease was conducted using a Protease Fluorescent Detection Kit (Sigma-Aldrich). The serine protease Rv0983c (pepD) was purified as a mycobacterial serine protease control [11]. The assay was done according to the manufacturer's instructions. Briefly, all of the test samples were incubated with incubation buffer (20 mM Na_3PO_4, 150 mM NaCl, pH 7.6) and FITC-casein (20 ng). After incubation, fluorescence intensity at the excitation and emission wavelengths of 485 and 535 nm were measured in the supernatant containing FITC-labeled fragments using a Multiskan Spectrum microplate spectrophotometer (Enspire, PerkinElmer, Waltham, MA, USA). All of the measurements were repeated in triplicate.

The substrates casein, gelatin, and milk were used to measure the protease activity of Rv3194c. PepD (50 μg), Rv3194c (50 μg), and Rv3194c (50 μg) with 10 μL of the Roche protease inhibitor cocktail, trypsin (10 μg), and 50 μL of 20 mM Tris-HCl were added to the plates of casein, gelatin, and milk, respectively. After incubation overnight at 37 °C, the protease hydrolytic substrate activity of Rv3194c was examined.

2.4. Effects of pH, temperature, divalent ions, and kinetic studies of Rv3194c

The effect of pH on Rv3194c serine protease activity was determined over a wide pH ranging from 3.0 to 12.0 (at 1.0 intervals) using Britton-Robinson buffer (20 mM acetic acid, 20 mM boric acid, and 20 mM hydrochloric acid, adjusted to the desired pH using 0.2 M NaOH) [12] as the reaction solution, following incubation at 37 °C for 1 h. The reactions were conducted at temperatures ranging from 30 °C to 50 °C (at 2 °C intervals) at an optimal pH of 8.0. All of the results were confirmed by 15% SDS-PAGE. Quantitative detection of Rv3194c activity was determined using a previously described method [13]. The total reaction volume was 100 μL. All of the test samples were co-incubated with 10 μg BSA (Ameresco, Solon, OH, USA) substrate in Britton-Robinson buffer at different temperatures and pH levels for 1 h. Then 20 μL of 50% (w/v) TCA was added to terminate the reaction, after which the mixture was chilled on ice for 15 min followed by centrifugation at 10,000 rpm for 5 min. The supernatant was collected to measure the increase at 280 nm (dA_{280}) using the Nanophotometer™ Peal Ultramicro UV–Vis spectrophotometer. One unit of enzymatic activity was defined as the amount of Rv3194c (per mg) that hydrolyzed the BSA substrate, causing an absorbance value increase of 0.001 at A_{280} per min.

Different divalent ions affect the activity of serine proteases [14]. To verify the effects of divalent ions on the activity of Rv3194c, BSA substrate (10 μg) with Rv3194c (10 μg) and 5 mM of eight different divalent metal ion salts ($MgCl_2$, $FeCl_2$, $MnCl_2$, $CaCl_2$, $BaCl_2$, $NiCl_2$, $CuCl_2$, and $ZnCl_2$) were mixed in Britton-Robinson buffer and incubated at an optimal temperature of 40 °C and pH of 8.0. The effects of the divalent ions were measured using the spectrophotometric method described above. The value of dA_{280} in the reaction of Rv3194c with BSA substrate was set as 100% protease activity, and the relative activity of the other samples was calculated according to the 100% specimen. Each assay was repeated at least three times.

The parameters of the Michaelis-Menten kinetic curve on Rv3194c were measured with UV spectrophotometry. Briefly, 10 μg Rv3194c protein was co-incubated for 1 h with varying concentrations of BSA substrate (0.03125, 0.0625, 0.125, 0.25, 0.5, 1, 1.5, 2, 2.5, 3, 3.5, 4, 4.25, 4.5, 4.75, 5, 5.25, 5.5, 5.75, 6, 6.25, 6.5, 6.75, 7, 7.25, 7.5, 7.75, 8, 8.25, 8.5, 9, 9.25, 9.5, 9.75, and 10 mg/mL) at 40 °C, pH 8.0 with 5 mM $CaCl_2$. Tris-HCl buffer at 20 mM (pH 8.0, containing 5 mM $CaCl_2$) was used as a negative control. A 20 μL volume of 50% TCA was used to terminate the reaction. The supernatant was measured at 280 nm. All of the samples were measured in triplicate.

2.5. Screening of Rv3194c inhibitors

Inhibitors of Rv3194c were screened using 20 types of traditional Chinese medicine (TCM) monomers (Genistein, Iris Flavonoids, Vitexin, Quercetin, Luteolin, Garbanzoin, Gallnut, Curcumin, Rutin, Arbutin, Saponin, Cedarin, Ferulic acid, Betulinic acid (50% dimethyl sulfoxide dissolved), Forsythiaside, Isoquercetin, Scutellarin, Han Huangqi, Verbascoside, and Baicalin (50% absolute ethanol dissolved)) and seven types of chemical inhibitors (pepstatin A, EDTA, leupeptin, aprotinin, dithiothreitol (DTT), PMSF, and Roche inhibitor cocktail (dissolved in sterile water)). All TCM monomers, EDTA, DTT, and PMSF were purchased from Sigma-Aldrich. Pepstatin A, leupeptin, and aprotinin were purchased from APExBio (Houston, TX, USA). Purified Rv3194c (10 μg) was co-incubated for 1 h with 0.5 mM TCM monomers or 5 mM chemical inhibitors at 40 °C, pH 8.0 with 5 mM $CaCl_2$; 10 μg BSA was then added, and the mixture was incubated for an additional 1 h. Next, 20 μL of 50% (w/v) TCA was used to terminate the reaction in a total volume of 100 μL. Measurement of Rv3194c activity with different inhibitors was conducted by spectrophotometry. SDS-PAGE was used to detect BSA hydrolysis.

2.6. Site-directed mutagenesis and circular dichroism

The pET22b-Rv3194c plasmid was used as a template for amplification by PCR with complementary mutagenic primer sequences (Supplementary Materials Table S2). A total of 12 recombinant protein mutants (A135G/V136A, V138A, N167A/L168A, D169A, Q170A/

F171A, T172A/A173G, L174A/L175A, S253A/G254A, S86A/G87A, D308A/S309A, D308A, and S309A) were purified, and their relative protease activities were measured using the aforementioned methods.

Circular dichroism of variable temperature (20 °C and 40 °C) was used to verify the correct fold and changes in temperature stability of Rv3194c and the 12 mutants. UV CD spectra, between 190 and 260 nm, were collected using a 1-mm quartz cuvette containing 250 μL of protein solution (1 μg protein dissolved in 20 mM Tris-HCl buffer (pH 6.0), with a data pitch of 0.1 nm, a bandwidth of 2.0 nm, and a scanning speed of 50 nm/min on a Chirascan spectropolarimeter (Applied Photophysics Ltd., UK). All of the specimens were analyzed in triplicate.

2.7. Subcellular localization of Rv3194c

To investigate the subcellular localization of Rv3194c in recombinant Ms (rMs), the *rv3194c* gene was cloned into the pMV261-AI-N shuttle vector to generate a pMV261-*rv3194c* recombinant plasmid. The plasmid was then electroporated into Ms to construct the Ms-261-Rv3194c rMs strain. The preparation of subcellular fractions of BCG and rMs was conducted as previously described [15]. All of the fractions were analyzed by Western blotting using an anti-Rv3194c protein polyclonal antibody. The cytoplasmic control protein, KatG (catalase peroxidase), was also detected via Western blot. The results were detected and recorded using a Li-Cor Odyssey imaging system (Li-Cor Biosciences, USA).

2.8. Cellular assays

The wound-healing assay was conducted using THP1-derived macrophages. The monolayer macrophages (2×10^5 cells/mL) were treated for 2 h with 10 μg/mL of Rv3194c and Rv3194cM (D308, S309). RPMI 1640 medium was substituted as the blank control. The cells were then scratched with sterile 10 μL pipette tips, washed three times with PBS, and incubated with FBS-free RPMI 1640 medium. The cell migration distance was detected by microscopy at 0 h, 12 h, and 24 h. Meanwhile, the extent of the wound width was calculated using ImageJ software. Each assay was repeated in triplicate.

A concentration of 5 μg standard protein (C5, C5a, C3, and C3b; Sigma-Aldrich) was co-incubated for 2 h with 5 μg of Rv3194c protein at 40 °C, pH 8.0, and 5 mM $CaCl_2$ in 20 mM Tris-HCl. The digestion of C5, C5a, C3, and C3b by Rv3194c was examined by SDS-PAGE. The chemotaxis assay was then conducted in a 6.5-mm transwell chamber (Corning, Corning, NY, USA). THP1 monocytes were seeded at a density of 1×10^5 cells/mL in the upper chamber with 300 μL FBS-free RPMI 1640, and the lower compartment contained 700 μL of RPMI 1640 with 10% FBS, 10 μg/mL C5a, 10 μg/mL C5a + Rv3194c, 10 μg/mL C5a + Rv3194cM, 10 μg/mL FMLP (chemotactic peptide), and 1% sterile PBS as chemoattractants. After incubation for 24 h, the upper compartment of the chamber, with no migrating cells, was removed, and the traversed membrane cells were counted by microscopy. Each assay was repeated three times.

Phagocytosis and phagocytosis inhibition were evaluated with the Rv3194c protein and rMs strains (Ms-261, Ms-261-Rv3194c Ms-261-Rv3194cM (D308, S309), respectively. Rv3194c and Rv3194cM proteins were added to THP1-derived macrophages (2×10^7 cells/mL) to a final concentration of 10 μg/mL. Rv3194c, pre-incubated with Roche protease inhibitor cocktail, was used as the positive control, and RPMI 1640 instead of Rv3194c served as the blank control. After incubation for 2 h, the medium was replaced with fresh RPMI 1640, and the cells were infected with the Ms strain at an MOI of 10:1. After a 6-h infection, the THP1 cells were washed three times with sterile PBS, lysed with 80 μL mild cell lysis buffer (Beyotime, Beijing, China), and centrifuged. The pellets were then re-suspended in 7H9 broth, and the cell suspension was spread onto 7H10 agar plates. The Ms colony-forming units (CFU) were counted after three days of cultivation. To verify the results, three rMs strains (Ms-261, Ms-261-Rv3194c, and Ms-261-Rv3194cM) were used to infect the THP1-derived macrophages. The growth curve measurement of rMs *in vitro* showed no significant changes in growth character among the rMs (Fig. S6A in supplementary materials). The CFU of the rMs was counted using the method above. All of the assays were done in triplicate.

2.9. Lung infection, pathological examination, and cytokine assays of mice

C57BL/6 mice were randomly separated into four groups and anesthetized with dry ice prior to bacterial infection. The rMs strains (1×10^8 CFU in 100 μL sterile PBS) were used to inoculate the mice via nasal administration. Three mice from each group were randomly euthanized at different time points (1, 7, 14, 21, and 28 d). The whole lungs of all of the challenged mice were removed, and the left lung was used for histopathological examination. The right lung was homogenized, and the lung slurry was spread onto 7H10 plates with 50 μg/mL kanamycin. After 3–4 d of incubation at 37 °C, the CFU of the rMs was calculated. The spleens were also taken from the euthanized mice at the above time points, and spleen lymphocytes were collected using the Mouse Spleen Lymphocyte Separation Kit (TBD, Tianjin, China). The spleen lymphocytes were stimulated overnight with 1×10^5 CFU/mL rMs strains. The secreted levels of IFN-γ, IL-1β, TNF-α, and IL-6 were examined in the supernatants using mouse IFN-γ, IL-1β, TNF-α, and IL-6 ELISA Kits (eBioscience, San Diego, CA, USA).

2.10. Statistical analysis

The data are expressed as the mean ± standard error of the mean (SEM). Significant differences were analyzed with one-way analysis of variance (ANOVA) and two-way ANOVA, followed by Bonferroni's multiple comparisons test. Statistical analysis of the data was performed using Prism 5.0 software (San Diego, CA, USA). *P* values were used to distinguish significant differences (* $0.01 < P < 0.05$, ** $P < 0.01$, *** $P < 0.001$).

3. Results

3.1. Expression, purification, and identification of Rv3194c

The *rv3194c* gene was cloned into pET22b vector and transformed into *E. coli*. In order to identify whether Rv3194c was expressed in *E. coli* and purify the Rv3194c protein *in vitro*, immunoblotting was used to analyze Rv3194c expression with anti-6xHis and anti-Rv3194c (Fig. 1A and B). SDS-PAGE analysis showed that the Rv3194c protein was present in inclusion body forms. The Rv3194c was subsequently re-natured and purified by Ni^{2+} affinity chromatography (Fig. 1C), gel filtration chromatography, and ion-exchange chromatography purification (Figs. S1A and B in Supplementary Materials). More than 98% of purified soluble protein was obtained. Subsequent mass spectrometry and peptide mass fingerprinting results showed that the expected protein, Rv3194c (Accession No. NP_217710.1), was obtained from MTB H37Rv (Fig. S1C in Supplementary Materials).

3.2. Specificity of Rv3194c serine protease activity

To verify the serine protease activity of purified Rv3194c, FITC-labeled casein and casein, milk, and gelatin agar plates were used to detect Rv3194c protease activity. Purified serine protease Rv0983c (pepD) (Fig. S2A–D in Supplementary Materials) was used as a mycobacterial serine protease control. The results indicated that Rv3194c protein could cleave the FITC-labeled casein substrate (Fig. 2A) and hydrolyze milk, casein, and gelatin, showing visible hydrolysis on the plates (Fig. 2B). These results indicated that Rv3194c has serine protease activity.

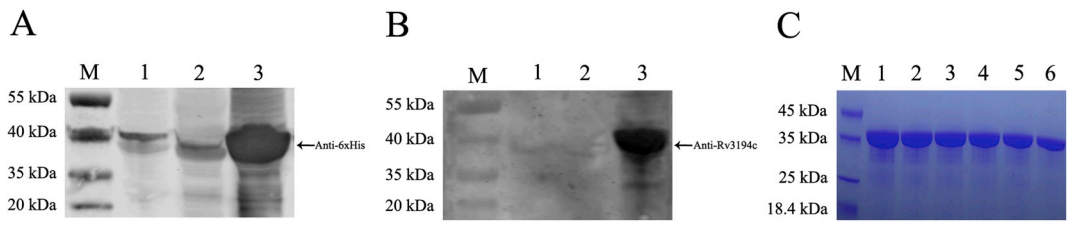

Fig. 1. Purification and identification of Rv3194c.
(A) and (B) Western blotting analysis of Rv3194c protein with anti-6 × His antibody and anti-Rv3194c. Line 1: induced empty vector pET-22b; Line 2: pET22b-Rv3194c without induction; Line 3: pET22b-Rv3194c with induction. (C) The affinity-purified Rv3194c protein was analyzed by SDS-PAGE. Purified Rv3194c protein was eluted by different imidazole concentration gradients. Line 1: 60 mM imidazole; Line 2: 100 mM imidazole; Line 3: 125 mM imidazole; Line 4: 150 mM imidazole; Line 5: 175 mM imidazole; Line 6: 200 mM imidazole; and Line M: protein molecular weight marker.

3.3. Effects of pH, temperature, and divalent ions, and kinetic study of Rv3194c

Optimal pH, temperature, and divalent metal ions are important to enzymatic function. The results of BSA hydrolyzation demonstrated that Rv3194c was able to tolerate a wide pH range of 6.0–12.0 (Fig. S3A in Supplementary Materials), with maximal protease activity at pH 8.0 (Fig. 3A). Furthermore, Rv3194c hydrolyzed BSA at temperatures ranging from 30 °C to 50 °C (Fig. S3B in Supplementary Materials) with an optimal temperature of 40 °C (Fig. 3B). The effect of different divalent ions on Rv3194c activity was calculated at 40 °C and pH 8.0. The enzymatic activity of Rv3194c increased nearly 148.77% and 71.15% in the presence of 10 mM $CaCl_2$ and 10 mM $MnCl_2$, respectively. The same concentrations of $FeCl_2$ and $MgCl_2$ had no significant effect on Rv3194c activity; however, Ba^{2+}, Ni^{2+}, Cu^{2+}, and Zn^{2+} inhibited Rv3194c activity by approximately 66.62%, 89.78%, 85.6%, and 97.58%, respectively (Fig. 3C). These results demonstrate that the optimal enzymatic activity conditions for Rv3194c are 40 °C, at pH 8.0 with Ca^{2+}.

The enzymatic kinetic parameters of Rv3194c serine protease were determined under conditions of pH 8.0 and 40 °C in a 5 mM $CaCl_2$ divalent ionic salt solution with BSA substrate. Michaelis–Menten enzyme dynamic assays showed a Km value of 1.428 ± 0.18 mg/mL, and the Vmax value was calculated to be 26.74 U/mg/min for BSA hydrolysis (Fig. 3D).

3.4. Screening of TCMs and chemical inhibitors of Rv3194c

To determine the inhibitors of Rv3194c, the proteolytic activity was evaluated in the presence of 20 types of TCM monomers and seven chemical inhibitors (Figs. S4A and B in Supplementary Materials). Betulinic acid (No. 14) had significant protease inhibitor activity with an inhibitory rate of nearly 40.5%, and the other TCM inhibitors had no inhibitory effects on Rv3194c activity (Fig. 4A). EDTA, leupeptin, aprotinin, PMSF, and Roche protease inhibitor cocktail also inhibited protease activity. The inhibitory rates of PMSF and Roche cocktail were 90.7% and 94.8%, respectively, and were much higher than the inhibitory rates of EDTA, leupeptin, and aprotinin compared to the control group (***$P < 0.001$; Fig. 4B). These results demonstrate that betulinic acid, PMSF, and Roche cocktail are efficacious inhibitors of Rv3194c protease activity.

3.5. Site-directed mutagenesis and circular dichroism (CD)

Twelve variant proteins were purified (Fig. S5C in Supplementary Materials), each with a single or double residue of the predicted residues. Examination of the enzymatic activity by cleaving FITC-labeled casein substrates (Fig. S5D in Supplementary Materials) and the relative activity of the 12 mutants showed that the Rv3194cM D308A/S309A mutant protein caused 70.2% loss of protease activity, and the single point mutant S309A was shown to play an important role in catalytic activity causing 69.91% of enzymatic activity loss. The double-point mutants S253A/G254A and S86A/G87A caused 40% and 30% loss of activity, respectively. The other eight substitutions (A135G/V136A, V138A, N167A/L168A, D169A, Q170A/F171A, T172A/A173G; L174A/L175A, and D308A) resulted in relative activity losses of 8%, 7%, 6.6%, 12%, 15%, 13%, 10%, and 3.3%, respectively (Fig. 5A). To determine the correct fold and stability of the secondary structural elements of Rv3194c and the 12 mutants, CD spectroscopy was performed over wavelengths ranging from 190 to 240 nm at 20 °C and 40 °C, at pH 6.0. The curves converged at 20 °C and 40 °C, between a wavelength of 200

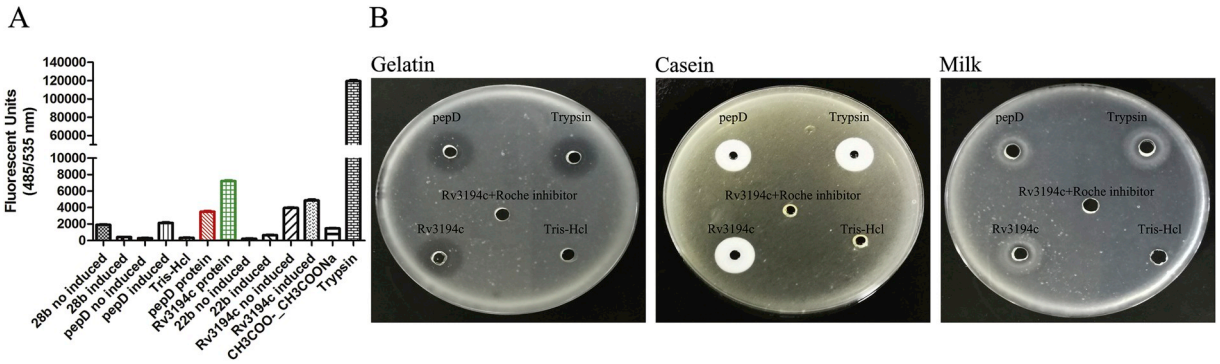

Fig. 2. Rv3194c hydrolyzes substrates and exhibits serine protease activity.
(A) Fluorescent detection of FITC-casein hydrolyzation by Rv3194c protein. The protease activity of Rv3194c was measured by cleaving FITC-labeled casein substrates, causing an increase of fluorescent units at excitation and emission wavelengths of 485 and 535 nm. The experimental samples, including Rv3194c, Rv0983c (pepD), supernatants of cellular lysis of induced or non-induced recombinant *E. coli* (pET22b-Rv3194c and pET28b-Rv0983c), and Trypsin-treated FITC-labeled casein were detected under the same conditions. All of the assays were replicated in triplicate. (B) Different substrate hydrolysis of Rv3194c was performed by the agar plate method. Tris-HCl, Rv3194c + Roche cocktail protease inhibitor served as a negative control. Rv0983c (pepD) and Trypsin served as a mycobacterial serine protease and positive control, respectively.

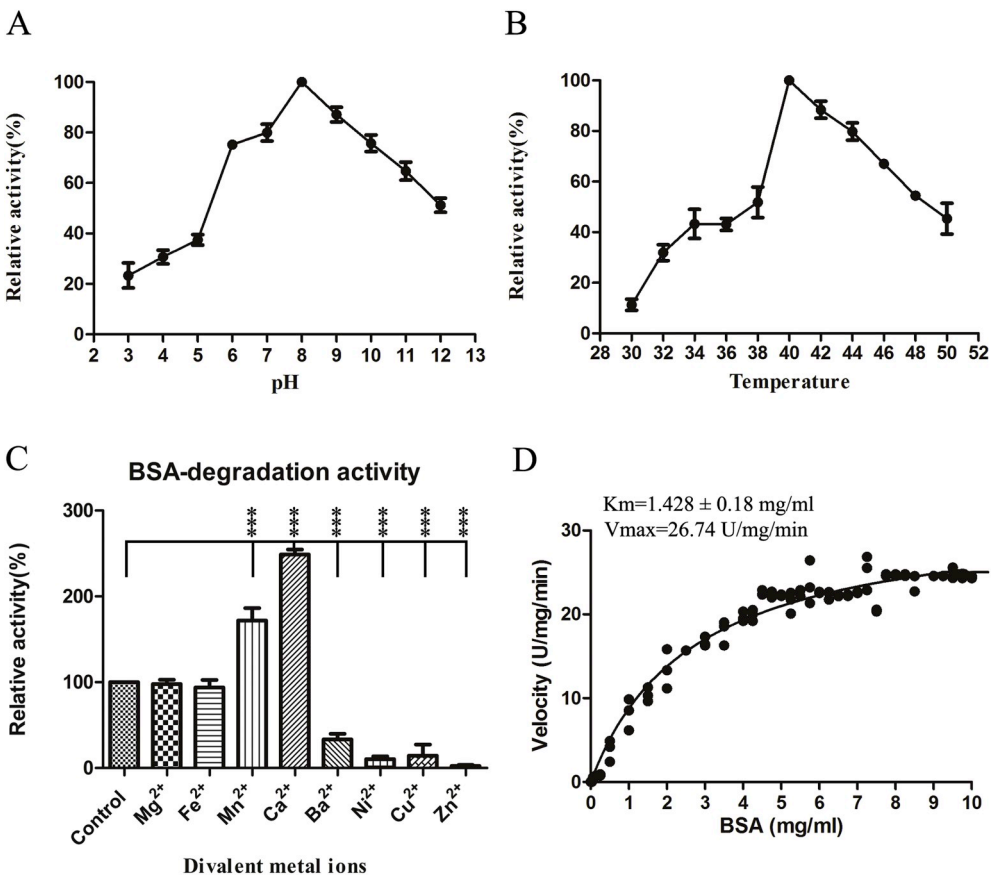

Fig. 3. Effect of pH, temperature, and divalent metal ions, and kinetic study on the protease activity of Rv3194c.
The effects of different pH, temperature, divalent metal ions, and kinetic study on the Rv3194c activity were evaluated by BSA hydrolyzation. (A) The different pH effect on Rv3194c serine protease activity was measured by the spectrophotometry method; error bars represent the SEM. (B) The effect of different temperatures on Rv3194c activity. (C) Effect of divalent metal ions on Rv3194c serine protease activity. One unit of Rv3194c enzyme activity was defined as the amount of Rv3194c (per mg) hydrolyzed substrate of BSA causing an absorbance value increase of 0.001 at A280/min at 40 °C with pH 8.0. Error bars represent SEM. (D) Michaelis-Menten kinetics analysis of serine protease activity of Rv3194c. Km value for BSA substrate hydrolyzation was 1.428 ± 0.18 mg/mL, and the Vmax value was 26.74 U/mg/min.

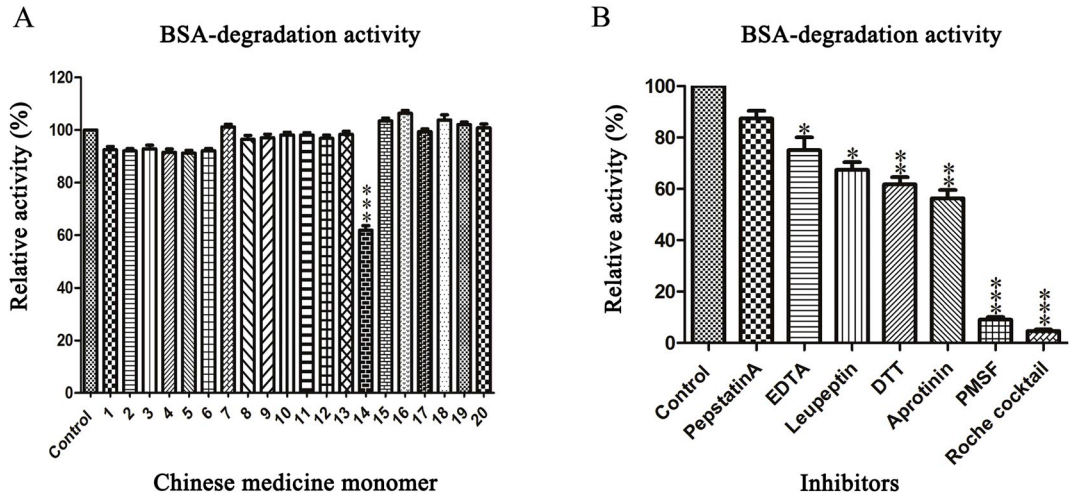

Fig. 4. Effects of TCMs and chemical inhibitors on Rv3194c activity.
(A) Quantitative analysis of TCM effect on Rv3194c activity. Control: Rv3194c + BSA; 1–20: Genistein; Iris Flavonoids; Vitexin; Quercetin; Luteolin; Garbanzoin; Gallnut; Curcumin; Rutin; Arbutin; Saponin; Cedarin; Ferulic acid; Betulinic acid; Forsythiaside; Isoquercetin; Scutellarin; Han Huangqi; Verbascoside; Baicalin. The relative activity of BSA hydrolyzation by the Betulinic acid monomer inhibitor was remarkably lower than other Chinese medicine monomers (***$P < 0.001$). (B) Quantitative analysis by spectrophotometry of the effect of chemical inhibitors on Rv3194c activity. Error bars represent SEM. The data were analyzed by two-way ANOVA, * $0.01 < P < 0.05$, ** $P < 0.01$, *** $P < 0.001$.

and 220 nm demonstrating a temperature stability of Rv3194c, efficacious mutant (D308A/S309A) (Fig. 5B) and the other 11 mutants (Fig. S7 in Supplementary Materials).

3.6. Subcellular localization of Rv3194c

Western blotting was conducted to investigate the subcellular localization of Rv3194c in rMs (Ms-261-Rv3194c) and BCG. The results demonstrated that Rv3194c was expressed in the total cell lysate, cell wall, cytoplasm, cell membrane, and cell culture filtrate in Ms-261-

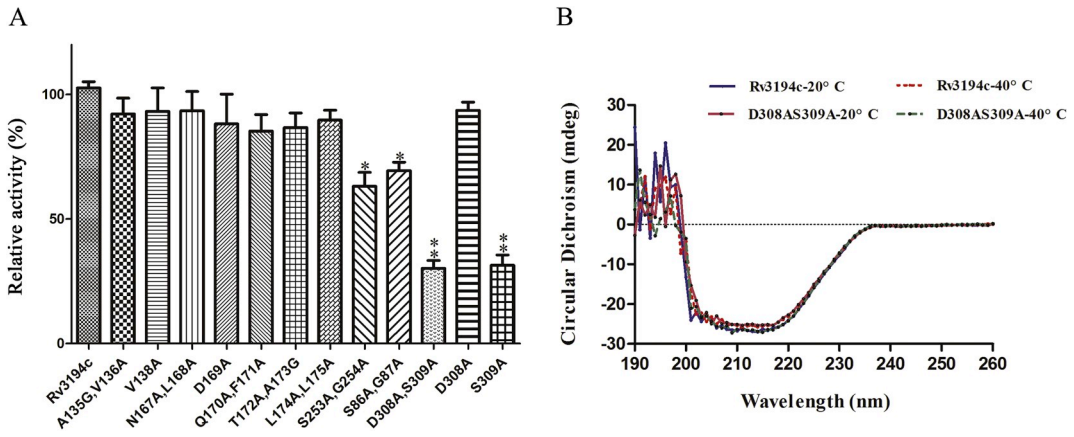

Fig. 5. Site-directed mutagenesis and circular dichroism.
(A) The relative activity of the site-directed mutants of Rv3194c. * $0.01 < P < 0.05$, ** $P < 0.01$. Error bars represent SEM. The data were analyzed by two-way ANOVA. (B) Circular dichroism assay of Rv3194c and Rv3194cM (D308A, S309A) at two different temperatures (20 °C and 40 °C).

Rv3194c (Fig. 6A). KatG, a cytoplasmic control protein, was only present in the total cell lysate and cytoplasm (Fig. 6A and B). Rv3194c had the same cellular localization in wildtype BCG cellular fractions, except for the cell culture filtrate (Fig. 6B). These data demonstrated that MTB Rv3194c is expressed in both the intracellular and extracellular contents in rMs and wild-type Rv3194c protein localized in the cell wall, cytoplasm, and cell membrane in BCG.

3.7. Wound healing assays in macrophages

A wound-healing assay was used to determine if Rv3194c affected macrophage migration. THP1-derived macrophages were treated with purified Rv3194c or the Rv3194cM protein. Migration was more inhibited in Rv3194c protein-treated THP1 macrophages at both 12 and 24 h than with Rv3194cM protein-treated (* $0.01 < P < 0.05$) and control groups (** $P < 0.01$; Fig. 7A). Wound width was also calculated using Image J software. The percentage of wound width was nearly 30.53% (Blank), 71.03% (Rv3194c), and 52.77% (Rv3194cM) at 12 h and 9.43% (Blank), 52.8% (Rv3194c), and 30.71% (Rv3194cM) at 24 h. The inhibitory migration rate of Rv3194c-treated cells was higher compared to Rv3194cM-treated cells (* $0.01 < P < 0.05$) and much higher compared to blank (** $P < 0.01$) (Fig. 7B), demonstrating that Rv3194c serine protease can inhibit migration of THP-1-derived macrophages.

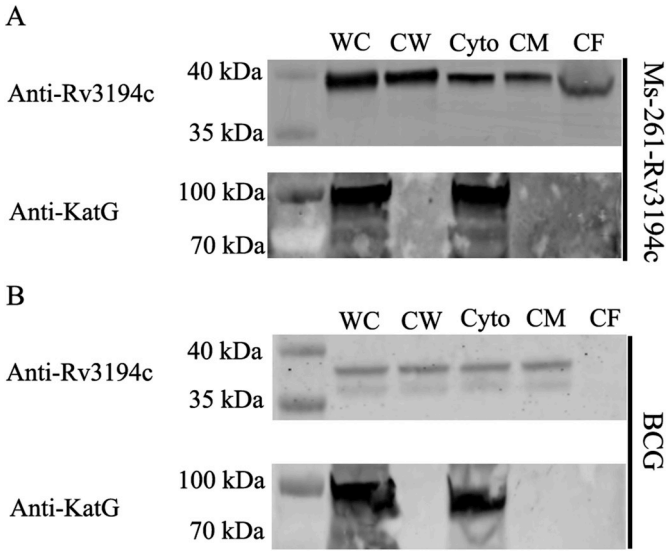

Fig. 6. Subcellular localization of Rv3194c.
Subcellular localization of Rv3194c in rMs strain and BCG were detected by Western blotting. Subcellular localization of Rv3194c in rMs (A) and BCG (B) strain. Whole-cell lysates (WC), cell wall (CW), cytoplasm (Cyto), cell membrane (CM), and cell culture filtrates (CF). KatG protein serves as a cytoplasm marker.

3.8. Chemotactic inhibition by C5a degradation and anti-phagocytosis by C3b digestion of Rv3194c

C5a is an important factor of complement components, which has a chemoattractive effect that can recruit macrophages to an infection site. The current study investigated whether Rv3194c could degrade C5a, thus indirectly causing inhibition of chemotaxis *in vitro*. The assay of C5 and C5a degradation demonstrated that Rv3194c could hydrolyze C5 and C5a *in vitro* by its protease activity (Fig. 7C). The transwell system assay showed that the number of cells with C5a treatment was higher than that with Rv3194c and Rv3194cM treatment (* $0.01 < P < 0.05$; Fig. 7D) demonstrating that C5a can recruit THP1 monocyte migration. There was no significant difference in cell number between C5a and FMLP treatments; however, cell number was lower with both C5a and FMLP treatments compared to treatment with the FBS control (* $0.01 < P < 0.05$; Fig. 7D). It was also found that Rv3194c can digest C3 and C3b α chain fragments (Fig. 7E). C3b plays an important role in phagocytosis as a component of the complement complex. Cellular phagocytosis of THP1-derived macrophages was evaluated to verify whether Rv3194c affected the cellular phagocytosis of mycobacteria. As mentioned above, purified Rv3194c protein was added to pre-cultured THP1-derived macrophages along with FBS. The THP1 macrophages were then infected with *M. smegmatis*. Phagocytosis of Ms by untreated THP1 macrophages was higher compared to THP1 macrophages treated with Rv3194c and Rv3194cM (*** $P < 0.001$); however, there was no significant difference when cells were pre-incubated with the cocktail inhibitor (Fig. 7F). To further confirm these results, THP1 macrophages were infected with three rMs (Ms-261-Rv3194c, Ms-261-Rv3194cM, and Ms-261) under the same conditions. The results demonstrated that the CFU/mL of Ms-261-Rv3194c and Ms-261-Rv3194cM was lower than that of Ms-261 at 12 and 24 h (* $0.01 < P < 0.05$; Fig. 7G). However, the CFU/mL of Ms-261-Rv3194cM was higher than the CFU/mL of Ms-261-Rv3194c at 6, 12, 24 and 36 h, although this difference was not significant. Taken together, these results show that Rv3194c can degrade C5a, causing chemotactic inhibition, and can digest C3b, thereby reducing phagocytosis by macrophages.

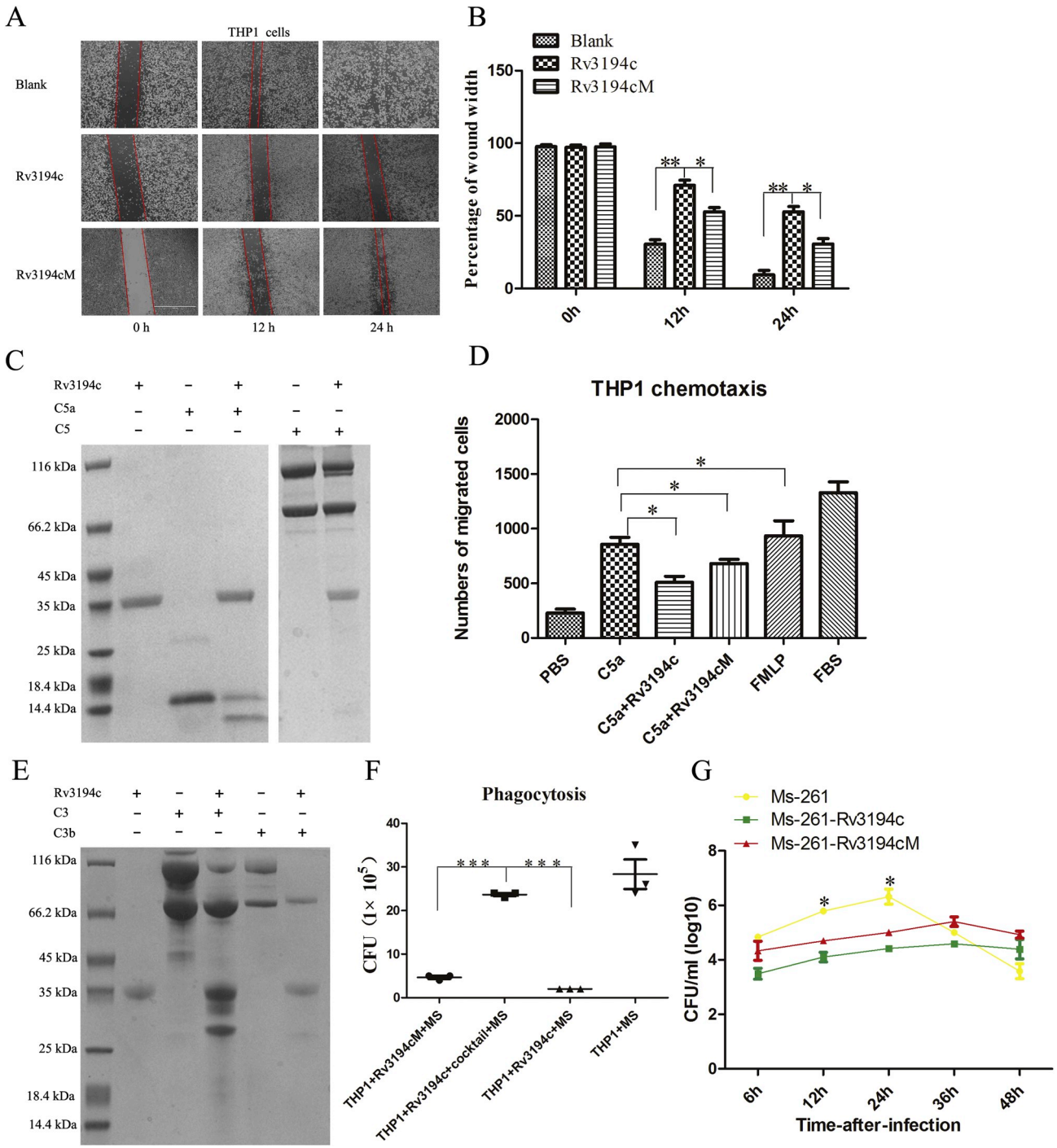

Fig. 7. Cellular assays verified Rv3194c protein function *in vitro*.
(A) The wound healing assays of Rv3194c- and Rv3194cM-treated THP1-derived macrophages at different time points (0, 12, 24 h). Blank group: THP1 macrophages were treated with 20 mM Tris-HCl, 150 mM NaCl, pH 8.0, 5 mM $CaCl_2$ at 40 °C. (B) The percentage of wound width was calculated with Image J software. Error bars represent SEM, * $0.01 < P < 0.05$, ** $P < 0.01$. (C) SDS-PAGE analysis of C5 and C5a degradation by Rv3194c *in vitro*. (D) Chemotactic inhibition by C5a degradation of THP1-derived macrophages, * $0.01 < P < 0.05$. (E) SDS-PAGE analysis of C3 and C3b digestion by Rv3194c *in vitro*. (F) THP-1-derived macrophages anti-phagocytosis of Ms by C3b digestion of Rv3194c, *** $P < 0.001$. (G) THP1-derived macrophages antiphagocytosis of rMs by C3b digestion of Rv3194c, * $0.01 < P < 0.05$. Each assay was repeated three times, and data analysis was conducted by two-way ANOVA.

3.9. Rv3194c promotes persistence in the lung and induces lung lesions

The lung is one of the main organs infected by MTB, and epithelial cells are target cells for adherence and invasion by mycobacteria [16]. To evaluate the function of Rv3194c in mycobacterial pathogenicity in mice, three rMs strains (Ms-261, Ms-261-Rv3194c, and Ms-261-Rv3194cM) were used to infect C57BL/6 mice. Bacterial load in the infected lung tissue was estimated at 1, 7, 14, 21, and 28 d after infection. There was no significant difference among the three groups 1 d after infection. However, the bacterial load was notably higher after infection with Ms-261-Rv3194c and Ms-261-Rv3194 cM at 7 d (** $P < 0.01$) and 14 d (*** $P < 0.001$) compared to Ms-261. Furthermore, bacterial loads in the lung tissues of the Ms-261 group mice were totally cleared 14 d after infection, whereas the bacterial load was not

completely cleared in Ms-261-Rv3194cM mice until 28 d after infection. Bacteria could still be detected at 28 d after infection with Ms-261-Rv3194c (Fig. 8A). Histological lesions in the immunized groups were examined 14 d after infection. No histological changes were detected in the PBS or Ms-261 groups. Lung tissues from the Ms-261-Rv3194cM group displayed mild inflammatory cell infiltration, whereas severe congestion and inflammatory cell infiltration were observed in the Ms-261-Rv3194c group (Fig. 8B). These results show that Rv3194c promotes Ms persistence in the lungs and induces lung lesions.

3.10. Rv3194c regulates inflammatory responses

To quantify the levels of inflammatory cytokines, IFN-γ, IL-1β, TNF-α, and IL-6 were measured in the supernatant of stimulated spleen lymphocytes. No significant changes in the levels of secreted IFN-γ were found in PBS- or Ms-261-infected mice at any time point (1, 7, 14, 21, and 28 d); however, IFN-γ levels were significantly higher in the Ms-261-Rv3194c group at 14 and 21 d compared to Ms-261-infected, PBS-infected (**$P < 0.01$), and Ms-261-Rv3194cM-infected (* $0.01 < P < 0.05$) mice. The high level of IFN-γ secretion in the Ms-261-Rv3194c group persisted 28 d after infection and was higher than levels in the Ms-261-Rv3194cM, Ms-261, and PBS groups (* $0.01 < P < 0.05$; Fig. 9A). IL-1β secretion in the Ms-261-Rv3194c group showed an increasing trend from 1 to 7 d, peaked at 14 d, and then decreased at 21 and 28 d after inoculation. The level of IL-1β in the Ms-261-Rv3194c group was significantly higher than that in the other three groups at 7 d (* $0.01 < P < 0.05$), 14 d (* $0.01 < P < 0.05$), and 21 d (***$P < 0.001$; Fig. 9B). A similar phenomenon was observed with TNF-α and IL-6. TNF-α levels in spleen lymphocytes treated with Ms-216-Rv3194c were markedly higher than those in the other groups at 7, 14, 21, and 28 d (***$P < 0.001$; Fig. 9C). The highest level of IL-6 secretion appeared at 7 d and decreased at 14 d; however, there was no significant difference among the four groups at 7, 21, and 28 d (Fig. 9D). These data show that Rv3194c can regulate inflammatory responses by upregulating the secretion of IFN-γ, IL-1β, TNF-α, and IL-6.

4. Discussion

Serine proteases are a large family of enzymes that exist in prokaryotic and eukaryotic organisms and possess important biological functions. The protease Esp regulates bacterial biofilm formation and inhibits nasal colonization of *Staphylococcus aureus*; Gp63 cleaves the NF-κB, p65 of macrophages, inducing chemokine expression; and PfSUB1 mediates the release of malaria parasites from host erythrocytes [17–20]. A considerable number of serine protease have been identified in pathogenic and non-pathogenic MTB due to their important biological significance [21,22]. However, until now, no evidence has been available regarding the identification and characterization of Rv3914c, the putative serine protease of the pathogenic MTB. To the best of our knowledge, the current study is the first to identify, characterize, and establish Rv3194c as a novel MTB serine protease, and to describe its physical and biochemical properties and immunomodulatory features.

The current study found an optimal temperature of 40 °C and an optimal pH of 8.0 for Rv3194c, similar to the previously reported temperature and pH values for the Sep1 serine protease from *Bacilus firmus* [23] and ScpA from *Alicyclobacillus sendaiensis* [13]. Furthermore, circular dichroism spectroscopy analysis demonstrated that Rv3194c and its 12 mutant proteins maintained a complete spectrum over a wide temperature range (20 °C−40 °C), showing that these proteins can stabilize their correct structural fold and tolerate widely varying temperatures, particularly 40 °C, which is consistent with the appearance of fever after MTB infection. This suggests that Rv3194c may contribute to the virulence of MTB. Although Fe^{2+} and Mg^{2+} had no significant influence on Rv3194c activity, Mn^{2+} and Ca^{2+} were found to promote the enzymatic activity of Rv3194c. This activity was inhibited by the divalent metal salt ions Cu^{2+} and Zn^{2+}. This may be because Rv3194c protease is denatured by heavy metal salts, which is a phenomenon found with Da-36 serine proteases in *Deinagkistrodon acutus* venom [24]. The effects of different ions on Rv3194c demonstrate that these divalent cations may bind to different amino acids to maintain enzymatic activity but are not important factors for integration with catalytic sites, such as in the *E. coli* protease Colicin E9 [25]. Moreover, Mn^{2+} and Ca^{2+} ions increased Rv3194c activity suggesting they play important roles in stabilizing the structure of the protease. The enzymatic activity of Rv3194c was strongly inhibited by the serine protease inhibitor PMSF (90%) [26] and the Roche protease inhibitor cocktail (94%). Meanwhile, EDTA, a divalent cations chelator, could chelate Ca^{2+} and showed a protease inhibitory effect on Rv3194c activity. Betulinic acid (40%) was first reported in this study as a TCM monomer that serves as an

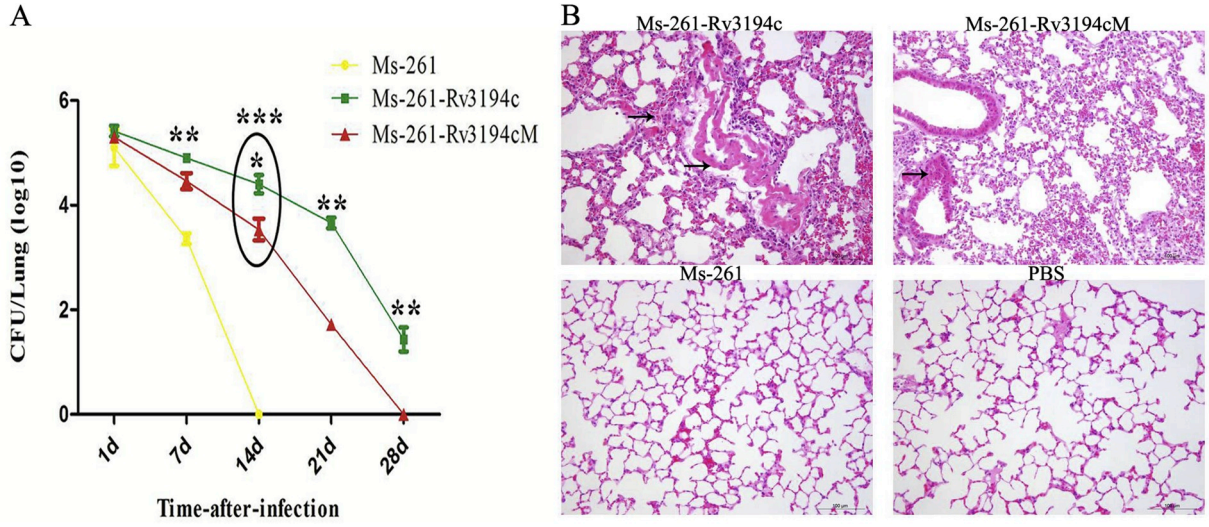

Fig. 8. Rv3194c promotes Ms persistence in the lung and induces lung lesions.
(A) Persistent rMs in mice lungs; bacterial loads in infected lung tissue from C57BL/6 mice, as transmitted by intranasal infection with Ms-261, Ms-261-Rv3194c, and Ms-261-Rv3194cM, were determined at 1, 7, 14, 21, and 28 d after infection. * $0.01 < P < 0.05$, **$P < 0.01$, and ***$P < 0.001$. (B) Histopathological examination of mice lungs; Ms-261-Rv3194c group: Severe hemorrhagic degeneration in alveolar epithelial cells and inflammatory cell infiltration. Ms-261-Rv3194cM group: Mild inflammatory cell infiltration. Ms-261 and PBS group: No pathological changes.

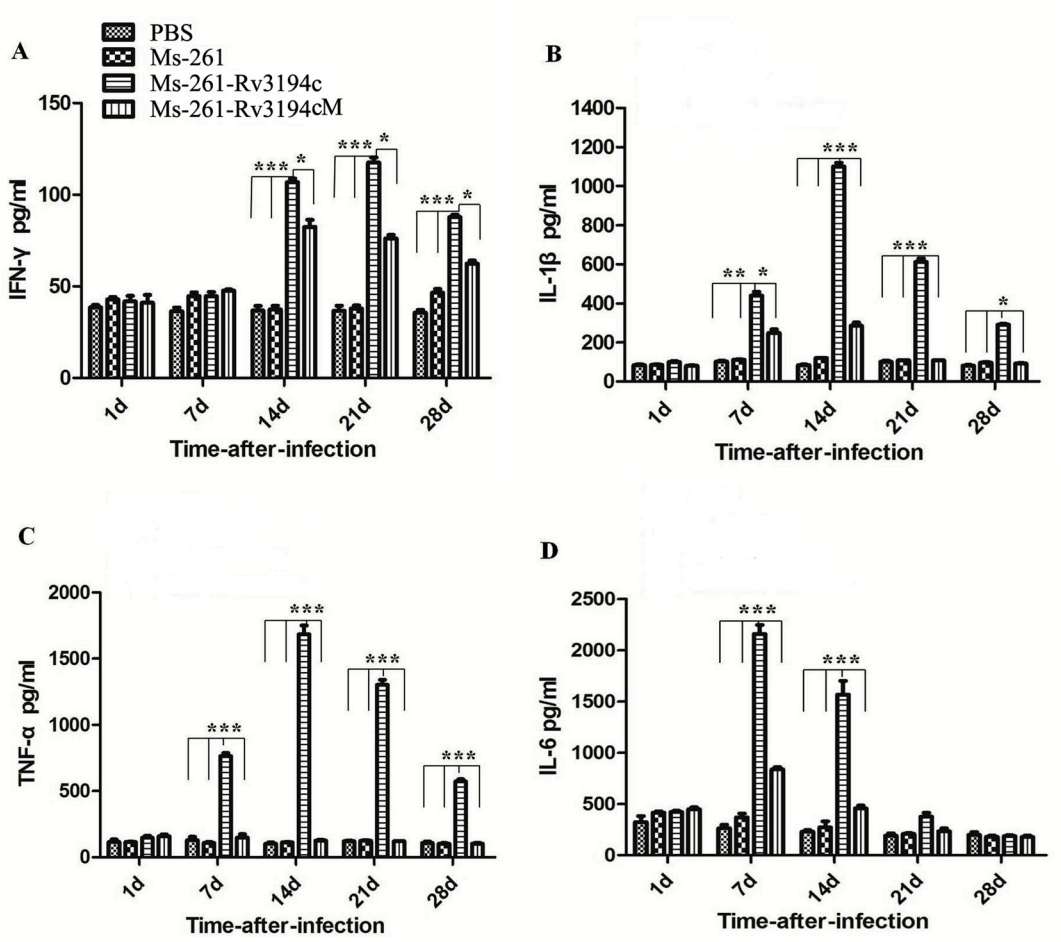

Fig. 9. Rv3194c upregulates the inflammatory responses of IFN-γ, IL-1β, TNF-α, and IL-6.
Quantitative analysis of inflammatory indicators in mice changed with rMs. The spleen samples of infected mice (n = 3 each group) were removed, and spleen lymphocytes were stimulated with PBS, Ms-261, Ms-261-Rv3194c, and Ms-261-Rv3194cM (D308A-S309A) *in vitro*. The secretion levels of cytokines were detected in the supernatant of cellular cultures. (A) Analysis of IFN-γ. (B) Analysis of IL-1β. (C) Analysis of TNF-α. (D) Analysis of IL-6. Two-way ANOVA followed by Bonferroni's multiple comparisons was used to analyze the data, $^{**}P < 0.01$ and $^{***}P < 0.001$.

effective inhibitor of mycobacteria serine protease. Furthermore, this natural product-based medicine was also found to have an inhibitory effect on the growth of Ms and Ms-261-Rv3194c (Figs. S6B and C in supplementary materials). Betulinic acid has also been found to increase anti-mycobacterial activity and has been considered to be an efficacious natural agent for mycobacteria therapy [27,28]. New studies on TCMs are currently ongoing to discover novel agents against drug-resistant pathogens. Therefore, the identification of new virulence factors and the screening of TCM inhibitors may be an effective method for developing new methods of treating TB [29].

Amino acid substitution studies indicated that D308 and S309, but especially the latter residue, may play an important role in Rv3194c serine protease activity, as the substitution of S309 caused a nearly 70% loss of Rv3194c serine protease activity. The importance of the residue substitution indicates that Rv3194c has a domain similar to the Asp/His/Ser catalytic triad, which is similar to that found in trypsin-like proteases [30]. C3b and C5a are important factors of complement components [31,32]. *In vitro* cellular assays demonstrated that Rv3194c could degrade C5a and digest C3b, causing inhibition of chemotaxis and indirectly inhibiting phagocytosis by THP1-derived macrophages, respectively. Rv3194c also inhibited the migration of macrophages, demonstrating that Rv3194c is an important mycobacterium virulence factor. Inflammatory cytokines, such as IFN-γ, can activate macrophage antimicrobial mechanisms against MTB. TNF-α is a crucial pro-inflammatory cytokine for MTB control in animals [33], contributing to the activation of macrophages to kill intracellular mycobacteria [34]. IL-6 is a cytokine that is critical for resistance against MTB but is not necessary to control the mycobacterial growth in infected loci after a low dose aerosol-delivered infection [35]. IL-6 is important for mediating inflammation in MTB infection but is not as essential as the TNF-α cytokine for anti-mycobacterial effector mechanisms [36]. IL-1β is another important pro-inflammatory cytokine, produced by macrophages, which is essential for killing MTB. Mice lacking IL-1β or the IL-1β receptor are highly susceptible to MTB infection. In addition, IL-1β directly inhibits the intracellular growth of MTB [37,38]. Here, we showed that Ms-261-Rv3194c rMs is capable of immunomodulating immunized mice spleen cells by inducing secretion of the pro-inflammatory Th1 cytokines TNF-α, IL-1β, IL-6, and IFN-γ, and observations in bacterial persistence and lung histopathology indicated that Rv3194c could significantly contribute to the TB immunopathology.

In summary, Rv3194c is a novel MTB serine protease that is associated with MTB pathogenicity. The current study provides the first biochemical and pathological analysis of the Rv3194c serine protease together with an *in vitro* immunized index detection of THP-1-derived macrophages and immunomodulatory responses elicited by the intact protease. Additional studies are needed to determine if the native Rv3194c in the original MTB strain plays a role in the virulence of mycobacterial infection. Rv3194c may be a novel target for the development of anti-mycobacterial drugs.

Author contributions

HL and SGL conceived and designed the experiments. HL completed the experiments, analyzed the data, and wrote the manuscript. GHD revised manuscript, and ZXW, HXL, and ZYC helped to finish the experiments. NNS and LPC provided some technical assistance during the experiments. The final version of the manuscript was approved by all the authors.

Declaration of competing interest

All the authors declare that this research was not in the presentation of any financial or commercial relationships that could lead to a potential conflict of interest.

Acknowledgments

The study was supported by the National Key Research and Development Project of China (2017YFD0500304). It was also granted from the National Natural Science Foundation of China (No. 31772740, No. 31772767, and No. 31873014).

Appendix A. Supplementary data

Supplementary data to this article can be found online at https://doi.org/10.1016/j.tube.2019.101880.

References

[1] WHO. The End TB Strategy. Global tuberculosis report 2018. Geneva, Switzerland: World Health Organization; 2018.
[2] WHO. The End TB Strategy. Global tuberculosis report 2016. Geneva, Switzerland: World Health Organization; 2016.
[3] Muttucumaru DG, Smith DA, McMinn EJ, et al. *Mycobacterium tuberculosis* Rv0198c, a putative matrix metalloprotease is involved in pathogenicity. Tuberculosis (Edinb) 2011;91:111–6.
[4] Ohol YM, Goetz DH, Cox JS, et al. *Mycobacterium tuberculosis* MycP1 protease plays a dual role in regulation of ESX-1 secretion and virulence. Cell Host Microbe 2010; 7:210–20.
[5] Makinoshima H, Glickman MS. Regulation of *Mycobacterium tuberculosis* cell envelope composition and virulence by intramembrane proteolysis. Nature 2005; 436:406–9.
[6] Skeiky YA, Mohamath R, Reed SG, et al. Cloning, expression, and immunological evaluation of two putative secreted serine protease antigens of *Mycobacterium tuberculosis*. Infect Immun 1999;67:3998–4007.
[7] Hu Q, Liu P, Jin M, et al. 44 Identification of a cell wall-associated subtilisin-like serine protease involved in the pathogenesis of *Streptococcus suis* serotype 2. Microb Pathog 2010;48:103–9.
[8] Fernaays MM, Lesse AJ, Murphy TF, et al. Characterization of igaB, a second immunoglobulin A1 protease gene in non-typeable *Haemophilus influenzae*. Infect Immun 2006;74:5860–70.
[9] Zhong G. *Chlamydia trachomatis* secretion of protease for manipulating host signaling pathways. Front Microbiol 2011;2:14.
[10] Zhao D, Lin L, Wen F, et al. Expression, purification and characterization of Rv3194c protein from *Mycobacterium tuber*culosis. Weishengwu Xuebao 2016;56: 1847–55.
[11] White MJ, Savaryn JP, Zahrt TC, et al. The HtrA-like serine protease PepD interacts with and modulates the *Mycobacterium tuberculosis* 35-kDa antigen outer envelope protein. PLoS One 2011;6:e18175.
[12] Dang G, Pang H, Liu S, et al. Expression, purification and characterisation of sectreted esterase Rv2525c from *Mycobacterium tuberculosis*. Appl Biochem Biotechnol 2015;176:1–12.
[13] Tsuruoka N, Nakayama T, Ashida M, et al. Collagenolytic serine-carboxyl proteinase from *Alicyclobacillus sendaiensis* strain NTAP-1: purification, characterization, gene cloning, and heterologous expression. Appl Environ Microbiol 2003;69:162–9.
[14] Hahn BS, Yang KY, Kim YS, et al. Purification and molecular cloning of calobin, a thrombin-like enzyme from *Agkistrodon caliginosus* (Korean viper). J Biochem 1996; 119:835–43.
[15] Vizcaíno C, Patarroyo ME, Patarroyo MA, et al. Computational prediction and experimental assessment of secreted/surface proteins from *Mycobacterium tuberculosis* H37Rv. PLoS Comput Biol 2010;6:e1000824.
[16] Russell DG. *Mycobacterium tuberculosis* and the intimate discourse of a chronic infection. Immunol Rev 2011;240:252–68.
[17] Kristjánsson MM, Asgeirsson B, Bjarnason JB. Serine proteinases from cold-adapted organisms. Adv Exp Med Biol 1997;415:27–46.
[18] Iwase T, Uehara Y, Mizunoe Y. *Staphylococcus epidermidis* Esp inhibits *Staphylococcus aureus* biofilm formation and nasalcolonization. Nature 2010;465: 346–9.
[19] Takaya A, Suzuki A, Yamamoto T, et al. Derepression of *Salmonella* pathogenicity island 1 genes within macrophages leads to rapid apoptosis via caspase-1- and caspase-3-dependent pathways. Cell Microbiol 2005;7:79–90.
[20] Staroscik AM, Denkin SM, Nelson DR. Regulationof the *Vibrio anguillarum* metalloprotease EmpA by posttranslational modification. J Bacteriol 2005;187: 2257–60.
[21] Sassetti CM, Boyd DH, Rubin EJ. Genes required for mycobacterial growth defined by high density mutagenesis. Mol Microbiol 2003;48:77–84.
[22] Ribeiro-Guimarães ML, Pessolani MC. Comparative genomics of mycobacterial proteases. Microb Pathog 2007;43:173–8.
[23] Geng C, Nie X, Peng D, et al. A novel serine protease, Sep1, from *Bacillus firmus* DS-1 has nematicidal activity and degrades multiple intestinal-associated nematode proteins. Sci Rep 2016;6:25012.
[24] Zheng Y, Ye FP, Lee WH, et al. Purification, characterization and gene cloning of Da-36, a novel serine protease from *Deinagkistrodon acutus* venom. Toxicon 2013; 67:1–11.
[25] Walker DC, Georgiou T, James R. Mutagenic scan of the H-N-H motif of colicin E9: implications for the mechanistic enzymology of colicins, homing enzymes and apoptotic endonucleases. Nucleic Acids Res 2002;30:3225–34.
[26] Quezada LA, Sajid M, McKerrow JH, et al. A blood fluke serine protease inhibitor regulates an endogenous larval elastase. J Biol Chem 2012;287:7074–83.
[27] Oloyede HOB, Ajiboye HO, Ajiboye TO, et al. Influence of oxidative stress on the antibacterial activity of betulin, betulinic acid and ursolic acid. Microb Pathog 2017;111:338–44.
[28] Rios JL, Manez S. New pharmacological opportunities for betulinic acid. Planta Med 2018;84:8–19.
[29] Dang G, Cao J, Liu S, et al. Characterization of Rv0888, a novel extracellular nuclease from *Mycobacterium tuberculosis*. Sci Rep 2016;6:19033.
[30] Ishida Toyokazu. Low-barrier hydrogen bond hypothesis in the catalytic triad residue of serine proteases: correlation between structural rearrangement and chemical shifts in the acylation process. Biochemistry 2006;45:5413–20.
[31] Abreu AG, Fraqa TR, Elias WP, et al. The serine protease Pic from *Enteroaggregative Escherichia coli* mediates immune evasion by the direct cleavage of complement proteins. J Infect Dis 2015;212:106–15.
[32] Del Tordello E, Vacca I, Serruto D, et al. *Neisseria meningitidis* NalP cleaves human complement C3, facilitating degradation of C3b andsurvival in human serum. Proc Natl Acad Sci USA 2014;111:427–32.
[33] Solovic I, Sester M, Milburn HJ, et al. The risk of tuberculosis related to tumour necrosis factor antagonist therapies: a TBNET consensus statement. Eur Respir J 2010;36:1185–206.
[34] Clay H, Volkman HE, Ramakrishnan L. Tumor necrosis factor signaling mediates resistance to mycobacteria by inhibiting bacterial growth and macrophage death. Immunity 2008;29:283–94.
[35] Sodenkamp J, Waetzig GH, Rose JS, et al. Therapeutic targeting of interleukin-6 trans-signaling does not affect the outcome of experimental tuberculosis. Immunobiology 2012;217:996–1004.
[36] Saunders BM, Frank AA, Cooper AM, et al. Interleukin-6 induces early gamma interferon production in the infected lung but is not required for generation of specific immunity to *Mycobacterium tuberculosis* infection. Infect Immun 2000;68: 3322–6.
[37] Jayaraman P, Dardalhon V, Hotta C, et al. Tim3 binding to galectin-9 stimulates antimicrobial immunity. J Exp Med 2010;207:2343–54.
[38] Jayaraman P, Nishimura T, Remold HG, et al. IL-1β promotes antimicrobial immunity in macrophages by regulating TNFR signaling and caspase-3 activation. J Immunol 2013;190:4196–204.